ACS OMEGA

Open Access

http://pubs.acs.org/journal/acsodf

Article

An Atomic-Scale Investigation of Liquid Crystal Orientation in Polar and Nonpolar Solvents

Nililla Nisoh, Nathanon Kerdkaen, Nattaporn Chattham, Mikko Karttunen, and Jirasak Wong-ekkabut*

Cite This: *ACS Omega* 2025, 10, 61288−61295

Read Online

ACCESS | Metrics & More | Article Recommendations | Supporting Information

ABSTRACT: Liquid crystals (LCs) exhibit unique ordered environments at interfaces, enabling functionalities in optical devices and biosensors. Their ability to transmit molecular interactions over macroscopic distances is well-known, yet the atomic-scale behavior of LC interfaces with polar and nonpolar solvents remains unclear. This study employs atomistic molecular dynamics (MD) simulations to investigate the orientation and structure of 4-cyano-4′-pentylbiphenyl (5CB) in vacuum, water, ethanol, and methane. Polar solvents promote the smectic phase but disrupt the molecular organization at interfaces through strong interactions with the nitrile group. Tilting of the 5CB molecules can be explained by density distributions and order parameters. In contrast, nonpolar solvents such as methane preserve the native ordering of 5CB, resulting in compact and parallel molecular arrangements with an increase in structural stability. These insights into solvent-induced structural stability and molecular orientation are crucial for optimizing liquid-crystal-based technologies.

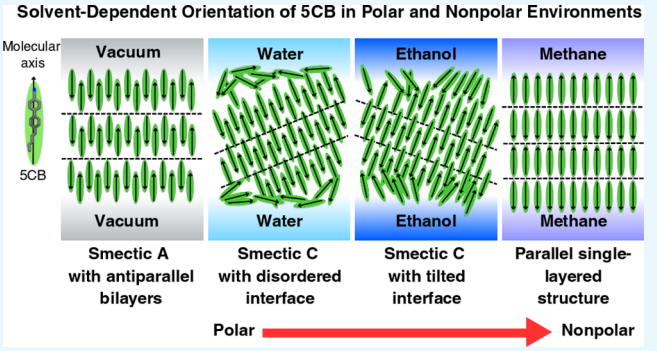

INTRODUCTION

Liquid crystals (LCs) are a distinct class of materials that exhibit long-range orientational order and maintain molecular mobility.[1] This combination of properties has enabled their widespread applications in technologies such as liquid crystal displays (LCDs),[2−4] advanced optical devices,[5,6] and biosensors.[7−9] A particularly significant feature of LCs is their ability to respond to external stimuli, including electric[10] and magnetic field.[11] The sensitivity of LCs to interfacial interactions makes them valuable for technologies that rely on controlled molecular alignment.[12,13]

Among thermotropic liquid crystals, 5CB has emerged as a model system for fundamental studies and practical applications, owing to its stable nematic phase at room temperature, and well-defined dielectric and optical anisotropies.[14] The molecular structure of 5CB, featuring a polar nitrile group attached to a biphenyl core (Figure 1), makes it especially sensitive to environmental conditions and interfacial phenomena. Experimental studies have shown that simple electrolytes and specific anions induce ordering transitions in 5CB at aqueous interfaces by modifying interfacial interactions.[15−17] Electrolytes produce an electrical double layer, causing an internal field to reorient the molecules,[15] whereas chaotropic anions interact with the nitrile group, resulting in a rapid planar-to-homeotropic transition.[16]

Despite the above advances, the molecular mechanisms underlying the LC orientation in solvents remain incompletely understood. MD simulations allow for investigation of LC behavior at the atomic scale enabling detailed characterization of the phase behavior, molecular orientation, and conformational dynamics.[18−21] Recent MD simulations have provided key insights into 5CB interfacial behavior, revealing molecular ordering and predicting anchoring energies.[12,22−27]

Computational studies have shown that the alignment of LCs at surfaces and interfaces may propagate through the bulk material, fundamentally affecting macroscopic properties. This bulk-interface relationship has been extensively studied, showing that surfaces can induce either homeotropic (perpendicular) or planar (parallel) alignment of the molecular axes extending the structural alignment deeply into the bulk region.[24,28] Specifically, Hadi et al.[26] have demonstrated that the distinct alignment patterns of 5CB depend on the type of the interface at which the hybrid alignment and planar alignment occur at vacuum and aqueous interfaces, respectively. This behavior has been attributed to the hydration of the polar nitrile group, highlighting the significant role of solvent polarity in determining LC orientation and anchoring strength. In addition, surface morphology has also been shown to play a crucial role in LC alignment. Chen et al.[27] reported that 5CB molecules confined between iron surfaces display different anchoring behaviors depending on surface structure; random planar

Received: June 11, 2025
Revised: November 27, 2025
Accepted: December 1, 2025
Published: December 9, 2025

https://doi.org/10.1021/acsomega.5c05516
ACS Omega 2025, 10, 61288−61295

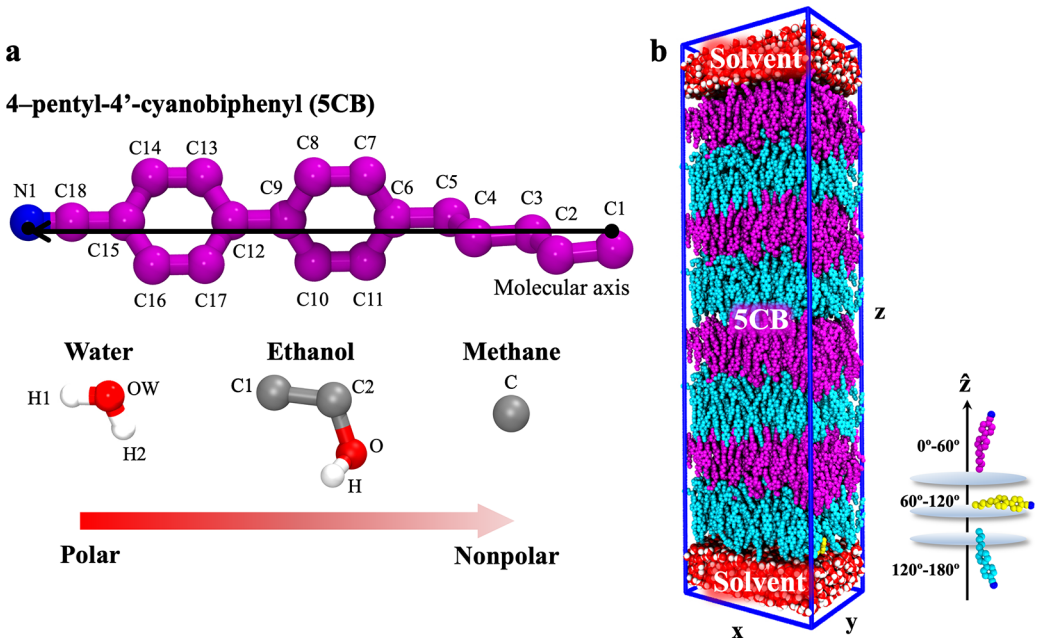

Figure 1. (a) The united atom models of 4-pentyl-4'-cyanobiphenyl (5CB) and solvent molecules. The carbon atoms of 5CB are shown in magenta and the nitrogen (N1) atoms in blue. The molecular axis of 5CB is the vector from C1 to N1. Oxygens are shown in red and hydrogens in white. In ethanol gray is used for the carbon atoms. Methane is shown as a single gray sphere. (b) Initial configuration of the 5CB molecules sandwiched between the water solvent layers along the *z*-axis. Color-coding corresponds to the molecular orientation angles (θ) with respect to the *z*-axis: 0°−60° (magenta), 60°−120° (yellow), and 120°−180° (cyan).

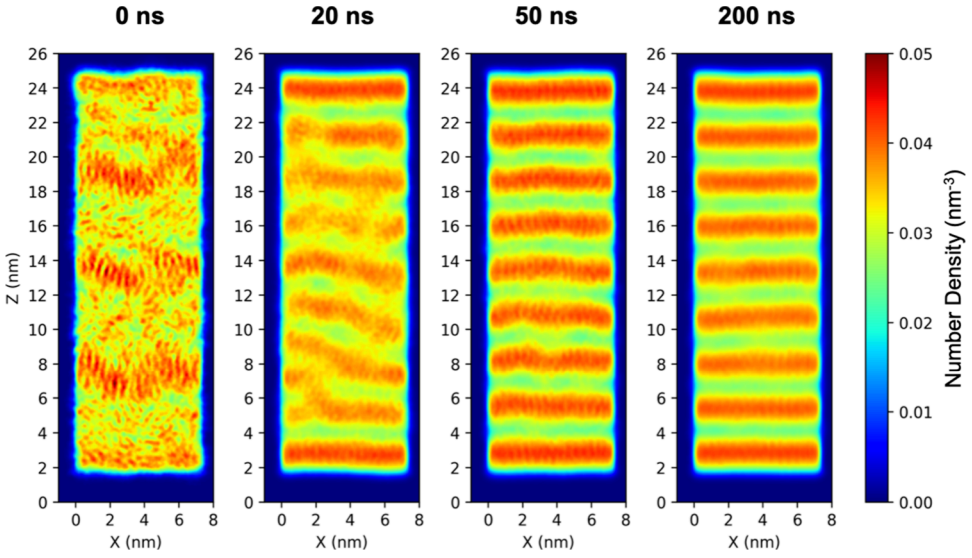

Figure 2. 2D density maps of the 5CB molecules in vacuum along the *x*−*z* plane at different simulation times: 0, 20, 50, and 200 ns. The density maps are colored by high density (red) or low density (blue). The maps show the development of smectic layering over time.

anchoring on flat surfaces versus unidirectional alignment on grooved surfaces.

Here, we employ atomistic MD simulations of 5CB in various solvent environments. By examining the behavior of 5CB in polar solvents (water, ethanol), nonpolar solvents (methane), and vacuum, we elucidate the fundamental mechanisms driving solvent-induced LC reorientation. Our investigation focuses on the key parameters including order parameters and density distributions to provide a comprehensive understanding of solvent-LC interactions at the molecular level. The insights gained from this study have significant implications for the development and optimization of LC-based technologies, particularly in applications where solvent interactions play a crucial role in device performance. Understanding how solvent polarity modulates LC behavior is essential for advancing the design of LC-based sensors, display technologies, and responsive optical systems.

METHODOLOGY

Molecular Dynamic (MD) Simulations. We used a united-atom molecular model to investigate the behavior of liquid crystals in different solvents with varying polarities, the molecules are shown in Figure 1a. The force field parameters of 5CB are based on Zhang et al.,[29] and the GROMOS 54a7 force field[30] was employed for the solvent molecules, simple

https://doi.org/10.1021/acsomega.5c05516
ACS Omega 2025, 10, 61288−61295

point-charge (SPC) water,[31] ethanol and methane. The simulated systems consisted of a slab of solvent molecules and layers of 5CB liquid crystals, as illustrated in Figure 1b. The initial configurations of the 5CB molecules were constructed as bilayer-like structures, stacked into four layers, with each bilayer comprising 512 molecules. In total, the systems had a fixed volume of 7.3 × 5.0 × 27.0 nm^3, and contained 2048, 4474, 3594, and 9856 of 5CB, water, ethanol, and methane, respectively. The difference in the numbers of solvent molecules is due to the solvent density. The molecular long axes of the 5CBs were aligned parallel to the z-direction. To eliminate possible overlaps that may have occurred during the setup, energy minimization was performed using the method of steepest descents. The simulations employed the NVT ensemble (constant number of atoms, volume and temperature), and the GROMACS 5.1.2 package[32] was used for all the simulations. The temperature was kept at 300 K using the v-rescale thermostat[33] with a time constant of 0.1 ps. A cutoff of 1.2 nm was used for both the Lennard-Jones and the short-range part of the electrostatic interactions. The long-range part of the Coulomb interactions was calculated using the particle-mesh Ewald (PME) method,[34,35] with reciprocal-space interactions evaluated on a 0.16 nm grid and cubic interpolation of order four. All bond lengths were constrained using the P-LINCS algorithm,[36] and the simulations were carried out for 200 ns with a time step of 2 fs. The last 50 ns of the trajectories were used for analysis. Periodic boundary conditions were applied in all three dimensions. The Visual Molecular Dynamics (VMD) software was used for rendering molecules.[37] The MDAnalysis,[38,39] numpy,[40] matplot[41] and scipy[42] libraries were employed for computing 2D density maps, 2D angle distributions and local order parameters.

RESULTS AND DISCUSSION

The Self-Organization of Liquid Crystal in the Vacuum. In Figure 2, 2D density maps of the 5CB molecules show the dynamic evolution of molecular organization in vacuum. At 0 ns, the distribution is irregular, indicating isotropic or disordered nematic phases. At 20 ns, layering begins to occur particularly at the interface regions. At 50 ns, the layers become more pronounced, and finally, at 200 ns, high-density smectic layers are observed.

The 2D density map at the end of simulation (Figure 3a) shows a well-defined layered structure of the 5CB molecules along the $x-z$ plane. The high-density regions correspond to molecular layers of interdigitation between the aromatic rings. To further analyze the molecular orientations, the angular distributions of the 5CB molecules (Figure 3b relative to the z-axis were analyzed. Two predominant angular ranges, $0° \leq \theta < 60°$ (purple) and $120° \leq \theta < 180°$ (cyan), indicate an antiparallel molecular alignment. This arrangement is well in agreement with the behavior of liquid crystals transitioning into the smectic-A phase as reported by Hadi et al.[12,26] The molecular snapshots in Figure 3c also confirm the spontaneous self-assembly of the 5CB molecules into antiparallel double layers. These layers are uniform across both the interfacial and the bulk regions, demonstrating the significant role of vacuum-induced alignment, driving the formation of the smectic-A phase. This finding highlights the importance of molecular organization in vacuum and at the 5CB-solvent interface. In addition, the structural distinction between the smectic A and smectic C phases can be briefly summarized as follows: In the smectic A phase, molecules are organized into well-defined layers and oriented perpendicular to the layer plane, leading to uniform parallel alignment to the normal plane-axis. In contrast, while the smectic C phase also forms layered structure, the molecular axes are tilted at a finite angle relative to the normal plane-axis. This distinction provides a useful framework for interpreting the solvent-induced changes in 5CB organization observed in our simulations. In the following section, we explore how the presence of solvents changes the phase and behavior of 5CB.

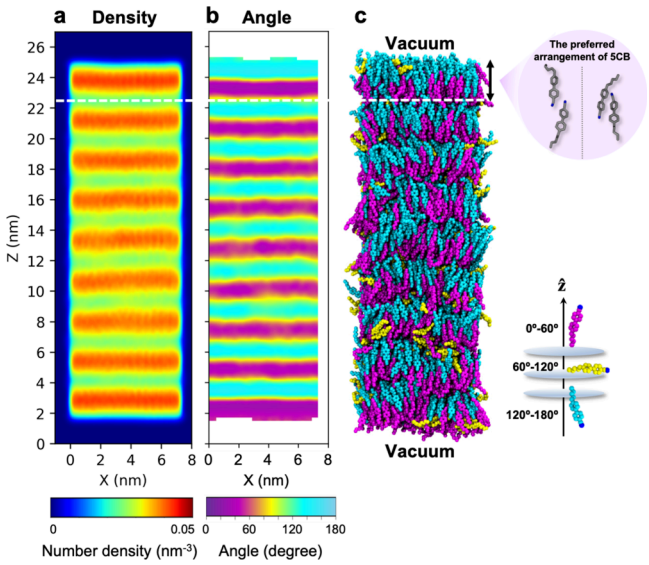

Figure 3. Visualizations of a 5CB liquid crystal system at 300 K in vacuum along the $x-z$ plane, with (a) 2D density map, (b) 2D angle distribution of the 5CB molecules, and (c) a molecular snapshot in vacuum after equilibration. The color-coding represents the variations in molecular orientation angles (θ): $0° \leq \theta < 60°$ (purple), $60° \leq \theta < 120°$ (yellow) and $120° \leq \theta < 180°$ (cyan). Density and angle plots were calculated after 150 ns of simulation.

Effects of Solvents on the Orientation of 5CB. The interface with vacuum plays a significant role in increasing the orientational order of the 5CB molecules, inducing a homeotropic alignment of the layers. To explore how the presence of a solvent affects the molecular organization, we investigated 5CB in three different solvents with varying polarities, water, ethanol, and methane. Figure 4 shows molecular snapshots (Figure 4a) and 2D density maps (Figure 4b).

In polar solvents, such as water and ethanol, the 5CB molecules show well-defined layers in the bulk region, indicating a smectic C-phase. These layers are characterized by interdigitated bilayers with antiparallel molecular orientations and a tilt relative to the layer normal. The density maps confirm the presence of a periodic structure, further supporting the formation of a smectic phase. Notably, in both water and ethanol, the molecules retain an organized and tilted configuration. In contrast, in methane, a nonpolar solvent, the 5CB molecules adopt a single-layered configuration with parallel molecular alignment instead of interdigitated bilayers. The density map reveals a more compact molecular arrangement, suggesting that nonpolar solvents promote a simpler and more ordered structure. The absence of a pronounced tilt compared to polar solvents highlights the role of solvent interactions in modulating 5CB alignment. These findings suggest that solvent polarity plays an important role in determining 5CB molecular organization.

https://doi.org/10.1021/acsomega.5c05516
ACS Omega 2025, 10, 61288−61295

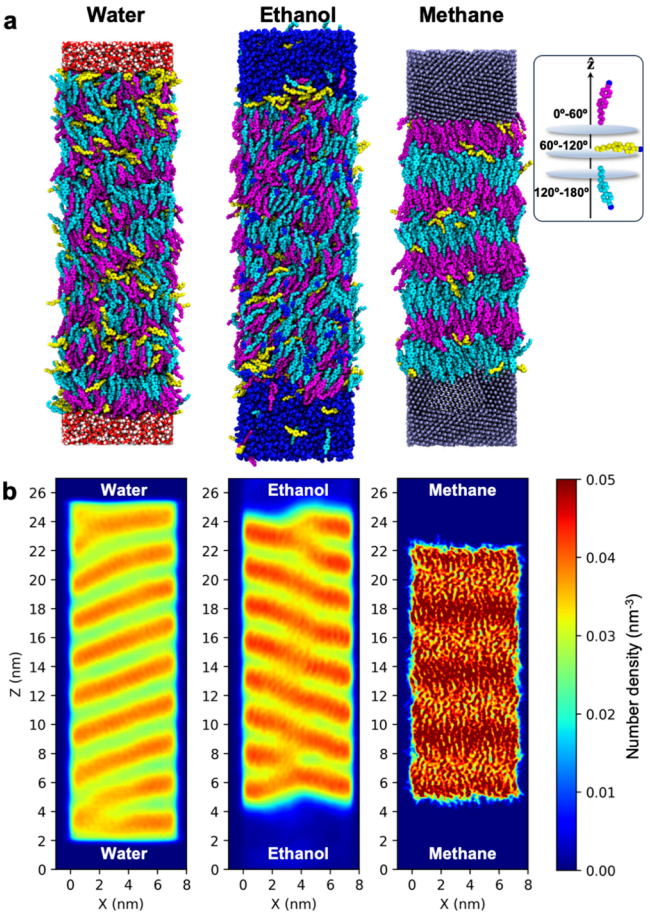

Figure 4. (a) Snapshots of molecular organization of 5CB in the water, ethanol and methane, after equilibration. Molecules are color-coded based on the angle relative to the z-axis. (b) 2D density maps of 5CB along the x−z plane.

Polar solvents facilitate the formation of interdigitated bilayers, while nonpolar solvents preserve simpler and nontilted arrangements. Although experimental studies on 5CB behavior in solvents are limited, the results align with the current observations of planar alignment at water interfaces, further reinforcing the impact of solvent interactions on liquid crystal structuring.[43] Specifically, we analyzed the molecular orientation relative to an axis normal to the solvent, and calculated the local order parameter by the Legendre polynomial $P_2(z)$ according to

$$\langle P_2(z)\rangle = \langle \frac{3}{2}\cos^2\theta - \frac{1}{2}\rangle \quad (1)$$

where $\langle\cdots\rangle$ denotes the ensemble average, and θ is the angle between the molecular axis of 5CB and the z-axis. In Figure 5, the local order parameter of the 5CB molecules in vacuum shows oscillatory behavior, with P_2 values ranging between 0.2 and 0.8. This oscillation corresponds to the formation of a highly ordered smectic phase along the z-direction. The regularity and magnitude of these oscillations indicate a strong orientational order in the absence of solvent, consistent with previous studies on liquid crystals in vacuum environments.[26] This highly ordered structure highlights the intrinsic tendency of the 5CB molecules to align along the z-axis in vacuum conditions.

In the water system, the $P_2(z)$ profile shows reduced oscillations in the bulk region, and the order parameter decreases to −0.4 near the water-5CB interface. This disruption

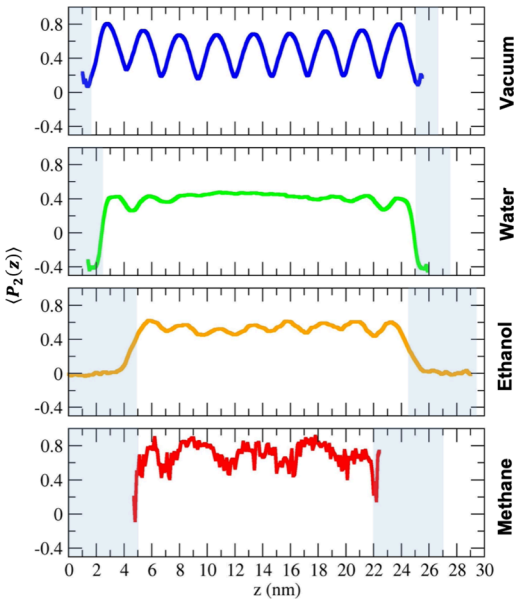

Figure 5. Local order parameter in different solvents along the z-direction. The blue-shaded areas indicate the solvent regions, while the unshaded regions correspond to the bulk 5CB liquid crystal.

at the interface is attributed to the strong interactions between the water molecules and the cyano (−CN) group of 5CB, including hydrogen bonding and dipole−dipole interactions. These interactions weaken the molecular alignment of 5CB, resulting in a reduced orientational order. These findings align with earlier observations by Ramezani-Dakhel et al.,[12,24] who reported a similar reduction in the 5CB order parameter at aqueous interfaces. In the ethanol system, the P_2 profile shows moderate oscillations, although less pronounced compared to the vacuum system. This indicates a partial retention of the smectic structure in the presence of ethanol. While the solvation effect of ethanol reduces the molecular order of 5CB to some extent, the bulk region still maintains a degree of molecular alignment. In the methane system, the $P_2(z)$ profile shows relatively stable oscillations throughout the bulk region, with a high degree of molecular ordering. Unlike polar solvents, methane has minimal perturbing effects on the orientational order of the 5CB molecules. This stability in the presence of methane suggests that nonpolar interactions exert less influence on the alignment of 5CB molecules compared to polar solvents.

Figure 6 presents contour maps of the probability distribution function P(z, cosθ) for the 5CB molecules, illustrating their angular distribution relative to the z-axis. Here, cosθ = −1 and +1 correspond to the molecular orientations with the cyano group pointing toward and away from the z-axis, respectively, while cosθ = 0 indicates a parallel alignment. In vacuum, the distribution shows sharp peaks at cosθ = ± 1, with a periodic pattern suggesting an antiparallel molecular arrangement. This indicates the formation of smectic layers throughout the 5CB phase, extending from the bulk region to the vacuum interface. The observed oscillatory behavior aligns with periodic variations in the order parameter $P_2(z)$ in eq 1, confirming the presence of a well-ordered smectic phase. In water, the molecular orientation distribution retains peaks at cosθ = ± 1, though less pronounced compared to vacuum. Additionally, a distinct peak at cosθ = 0 near the water-5CB interface suggests disordered molecular orientations at the boundary, reflecting solvent-induced disruption. In ethanol, the contour maps

https://doi.org/10.1021/acsomega.5c05516
ACS Omega 2025, 10, 61288−61295

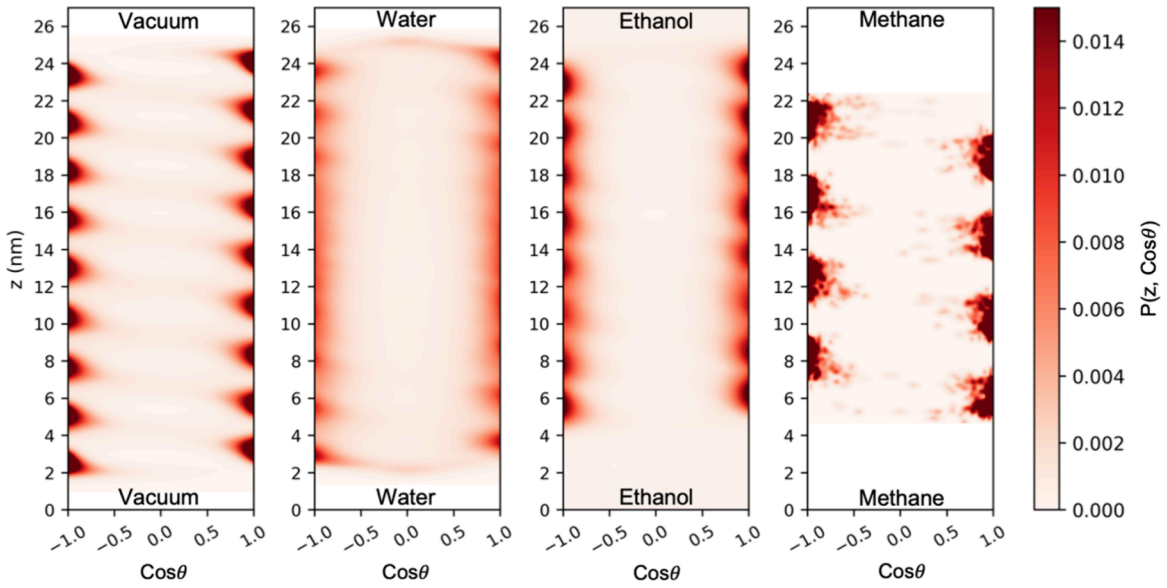

Figure 6. Contour map of the probability distribution function P(z, cosθ) for 5CB in the different solvents. The angle θ is the angle between the 5CB molecular axis and the z-direction.

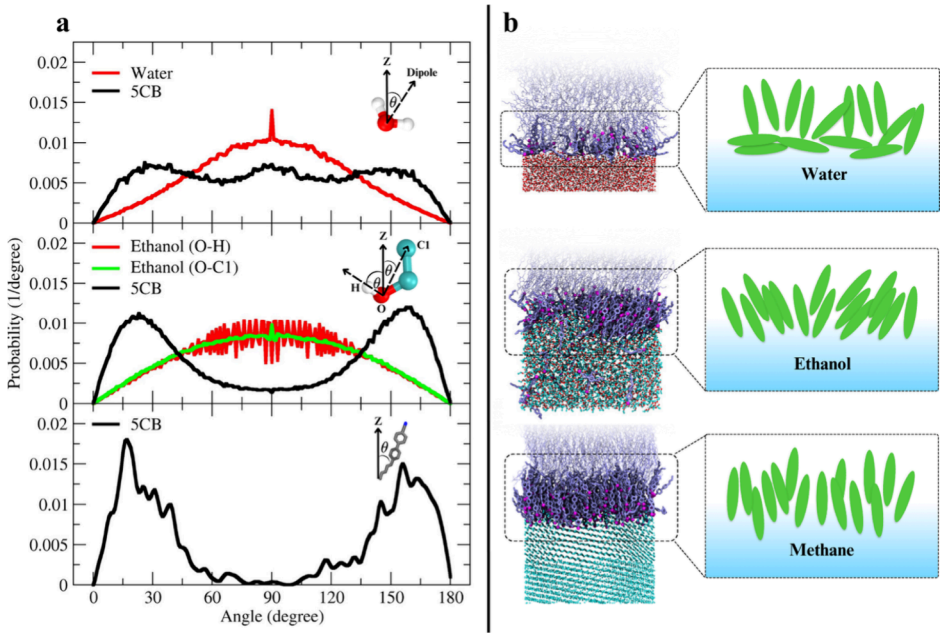

Figure 7. (a) Angle distributions of the 5CB and solvent molecules at the interface region depicting the probability as a function of the angle (θ) with respect to the z-axis for the 5CB and solvent molecules (water and ethanol). (b) Molecular snapshots and schematic illustrations of 5CB alignment at the interface region in the presence of water, ethanol, and methane solvents.

display peaks at cosθ = ± 1 throughout the entire 5CB film, indicating retained smectic-like structure. However, these peaks are more concentrated and periodic than in water. This suggests that ethanol partially disrupts, but does not eliminate, smectic order. In methane, the P(z, cosθ) profile is highly concentrated and uniformly distributed. The absence of distinct disruptions or irregularities indicates that the liquid crystalline structure remains well-preserved. Nonpolar solvents, here methane, maintain the 5CB molecular organization more effectively than polar solvents.

Our analysis of molecular orientation is related to the amphiphilic nature of 5CB and its specific interactions with solvents of varying polarities. Solvent polarity emerges as a key factor influencing the molecular alignment. Polar solvents disrupt ordering by interacting with the polar nitrile group of 5CB, leading to tilting that minimizes interfacial energy. Nonpolar solvents allow molecules to retain native ordering due to weaker solvent interactions. These observations are corroborated by the time evolution of the P_2 order parameter eq 1 (Figure S1), highlighting consistently high order in methane throughout the simulation.

Polar Solvents Induce a Disordered Phase. To investigate the mechanism behind polarity-induced disorder, we analyzed the angular distributions of both the 5CB and the solvent molecules at the interface (Figure 7). The interface region was defined as the spatial zone where the density profiles

https://doi.org/10.1021/acsomega.5c05516
ACS Omega 2025, 10, 61288−61295

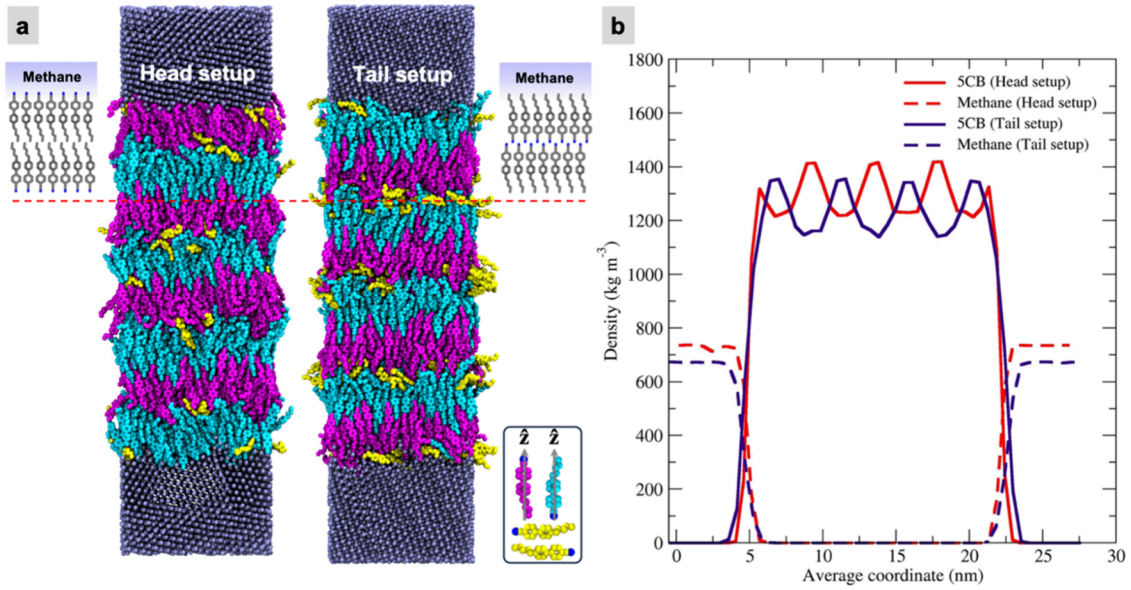

Figure 8. (a) The final configurations of the 5CB molecules interacting with methane with two different setups: the head setup (cyano group to methane) and the tail setup (alkyl chain to methane). (b) The density profiles of the 5CB and methane molecules in different setups along the *z*-axis.

of the 5CB and solvent molecules overlap. With water as the solvent (Figure 7a), the angle distribution of the water molecules shows a sharp peak around $\theta \approx 90°$. For 5CB, three prominent peaks are observed at approximately 30°, 90° and 150°. Notably, the 5CB peak at $\theta \approx 90°$ corresponds to a perpendicular orientation relative to the *z*-axis. This observation suggests that some of the 5CB molecules align with the highly polar water molecules. The strong polar interactions between the water molecules and the 5CBs drive significant molecular reorientation, disrupting the smectic layers and resulting in disordered molecular alignment, as illustrated in the schematic in Figure 7b. This disruption can be directly attributed to maximizing favorable solvent-nitrile interactions. Previous atomistic simulations by Ramezani-Dakhel et al.[12] provide a quantitative explanation for this phenomenon, their calculations of the molecular orientation free energy show that the cyano headgroup of 5CB is preferentially hydrated, and the hydrophobic tail favor to stay at the interface. They reported that the most favorable orientation corresponds to a tilt of ∼ 80° relative to the surface normal. Departures from this configuration to a tilt angle of ∼ 0° required a free energy penalty of about 4 kcal mol^{-1} (∼7kT). This energetic stabilization drives the interfacial 5CB molecules to reorient in order to maximize favorable solvent−nitrile interactions, thereby disrupting the uniform smectic layering observed in the bulk. In our simulations, this mechanism is manifested by the reduction in $P_2(z)$, broadening of the angular distributions, and the emergence of molecules oriented parallel to the interface ($\theta \approx 90°$). In the ethanol system, the angular distribution of the ethanol molecules, characterized by the O−H and O−C1 orientations, appears slightly broader. The 5CB molecules at the interface region display moderate ordering, with a relatively narrow peak and the absence of a central peak at $\theta \approx 90°$, in contrast to the water system. This indicates that the 5CB molecules at the ethanol interface do not align perpendicularly to the *z*-axis as they do in water. Instead, the lower polarity of ethanol leads to reduced disruption of the smectic phase, allowing for a more stable molecular arrangement. Interestingly, the 5CB molecules at the ethanol interface adopt a tilted angular orientation. With methane as the solvent, the 5CB angle distribution shows sharp peaks around 16° and 160°, reflecting strong alignment and a well-preserved liquid crystalline structure. This finding highlights the minimal effect of nonpolar solvents such as methane on the layer structure of 5CB molecules.

To ensure that the observed 5CB orientation in methane was not an artifact of the initial configuration with the cyano group directed toward the methane phase (the head setup, Figure 8a), additional simulations were conducted with the alkyl chain facing methane (the tail setup, Figure 8a). In both configurations, the 5CB molecules showed a pronounced layered arrangement, indicative of stable liquid crystalline order. The structural organization in both setups, as shown in Figure 8a, revealed negligible deviations, suggesting that the interaction of 5CB with methane is independent of the molecular orientation at the interface. Density profiles along the *z*-axis (Figure 8b) further support the observed structural stability. Both the head and tail setups display similar density patterns, with peak values around 1400 kg/m^3. Notably, the head setup exhibited slightly higher 5CB density. This can be attributed to stronger dipole−dipole interactions between the polar cyano groups and the methane interface, resulting in more compact molecular packing. In contrast, the nonpolar alkyl chains have weak interactions with methane, resulting in a slightly less packed molecular configuration. The periodic nature of the peaks reflects the characteristic lamellar organization of liquid crystals. Methane density profiles showed uniform distribution close to the 5CB layers, indicating minimal penetration of methane into the liquid crystal phase. The consistent ordering across both configurations implies that the weak van der Waals interactions between methane and 5CB do not significantly perturb the 5CB internal structure. This behavior can be attributed to the nonpolar nature of methane, which interacts similarly with both the cyano head and the alkyl tail of 5CB, thus exerting negligible influence on the overall molecular orientation. These findings demonstrate that 5CB's orientational order is stable in nonpolar system, regardless of the initial molecular alignment.

https://doi.org/10.1021/acsomega.5c05516
ACS Omega 2025, 10, 61288−61295

The experimental observation that at aqueous-facing nematic interfaces the addition of the interfacial solvent with surfactants and ions can drive the anchoring transitions and induce nematic wetting layers[16,17,43,44] aligns well with our simulation results. These experimental evidence support our simulation findings that polar headgroups and interfacial fields bias the orientation of 5CB molecules. Direct measurements using X-ray reflectivity and ellipsometry/optical techniques[17,44,45] have quantitatively characterized nematic ordering at LC/water interfaces, demonstrating chemistry-controlled anchoring transitions (planar ↔ homeotropic) and nematic wetting phenomena near the nematic−isotropic transition temperature (T_{NI}). Furthermore, experimental studies of solvent−LC systems show that dilution with small molecules such as methanol[46] and toluene[47] can effectively tune T_{NI} and interfacial responses, reinforcing our interpretation that specific solvation and interfacial polarity are crucial factors in modulating orientational states.

CONCLUSIONS

This study highlights the critical role of solvent polarity on the orientational order and dynamic behavior of 5CB liquid crystals. Through atomic-level molecular dynamics simulations, we found that water and ethanol induce a smectic-C phase layer. The strong interactions of the polar solvents with the nitrile groups of 5CB result in molecular tilting, and a decrease in orientational order. In contrast, methane preserves the native layered structure, and maintains the compact and parallel molecular arrangements. Significant differences in layer formation were observed in which the polar solvents promote interdigitated and antiparallel bilayers but the nonpolar solvent induces simpler and single-layer configurations. In addition, the diffusion analysis showed high molecular mobility in polar environments. On the other hand, significant confinement, reflecting a transition to a more rigid, ordered state is observed with the nonpolar solvent. These results help our understanding of the effect of solvent on liquid crystal. The polar solvents destabilize liquid crystalline order, whereas the nonpolar solvents maintain structural integrity. While our study focused on 5CB as a representative liquid crystal, the structural principles identified here are broadly relevant to other cyanobiphenyl homologues (nCB, n = 6−8) and amphiphilic mesogens. In particular, the interplay between the polar functional groups and solvent polarity can be exploited in molecular design to either destabilize or stabilize liquid crystalline ordering at interfaces. This insight bridges simulations with experimental observations, and highlights design strategies for optimizing LC-based sensors, optical devices, and composite materials across various solvent environments.

ASSOCIATED CONTENT

Supporting Information

The Supporting Information is available free of charge at https://pubs.acs.org/doi/10.1021/acsomega.5c05516.

The orientational order parameters as a function of time for 5CB with different solvents (Figure S1) (PDF)

AUTHOR INFORMATION

Corresponding Author

Jirasak Wong-ekkabut − *Department of Physics, Faculty of Science and Computational Biomodelling Laboratory for Agricultural Science and Technology (CBLAST), Faculty of Science, Kasetsart University, Bangkok 10900, Thailand;* orcid.org/0000-0002-3651-9870; Email: jirasak.w@ku.th

Authors

Nililla Nisoh − *Department of Physics, Faculty of Science and Computational Biomodelling Laboratory for Agricultural Science and Technology (CBLAST), Faculty of Science, Kasetsart University, Bangkok 10900, Thailand*

Nathanon Kerdkaen − *Department of Physics, Faculty of Science and Computational Biomodelling Laboratory for Agricultural Science and Technology (CBLAST), Faculty of Science, Kasetsart University, Bangkok 10900, Thailand*

Nattaporn Chattham − *Department of Physics, Faculty of Science, Kasetsart University, Bangkok 10900, Thailand*

Mikko Karttunen − *Department of Chemistry and Department of Physics and Astronomy, The University of Western Ontario, London, ON N6A 3K7, Canada; ELLIS Institute Finland, Espoo 02150, Finland; Department of Technical Physics, University of Eastern Finland, Kuopio FI-70211, Finland;* orcid.org/0000-0002-8626-3033

Complete contact information is available at: https://pubs.acs.org/10.1021/acsomega.5c05516

Notes

The authors declare no competing financial interest.

ACKNOWLEDGMENTS

This research has received funding support from the National Science, Research and Innovation Fund (NSRF) via the Program Management Unit for Human Resources & Institutional Development, Research and Innovation [grant nos. B13F660122, B11F670109, and B42G670041], the Postdoctoral Fellowship from Kasetsart University and Faculty of Science Kasetsart University. M.K. thanks the Canada Research Chairs Program. the Natural Sciences and Engineering Research Council of Canada (NSERC) and Foundation PS for financial support.

REFERENCES

(1) De Gennes, P.-G.; Prost, J. *The physics of liquid crystals*, 2nd ed.; Oxford university press, 1993.

(2) Hoogboom, J.; Rasing, T.; Rowan, A. E.; Nolte, R. J. LCD alignment layers. Controlling nematic domain properties. *J. Mater. Chem.* **2006**, *16*, 1305−1314.

(3) Schadt, M. Liquid crystal materials and liquid crystal displays. *Annual Reviews, Inc.* **1997**, *27*, 305−379.

(4) Chen, R. H. *Liquid crystal displays: fundamental physics and technology*; Wiley: Hoboken, NJ, 2011.

(5) Woliński, T.; Ertman, S.; Lesiak, P.; Domański, A.; Czapla, A.; Dąbrowski, R.; Nowinowski-Kruszelnicki, E.; Wójcik, J. Photonic liquid crystal fibers — a new challenge for fiber optics and liquid crystals photonics. *Opto-Electron. Rev.* **2006**, *14*, 329−334.

(6) Prasad, S. K.; Madhuri, P. L.; Satapathy, P.; Yelamaggad, C. A soft-bent dimer composite exhibiting twist-bend nematic phase: Photo-driven effects and an optical memory device. *Appl. Phys. Lett.* **2018**, *112*, No. 253701.

(7) Brake, J. M.; Daschner, M. K.; Luk, Y.-Y.; Abbott, N. L. Biomolecular interactions at phospholipid-decorated surfaces of liquid crystals. *Science* **2003**, *302*, 2094−2097.

(8) Das, S.; Chakraborty, R.; Kula, P.; McLaughlin, J.; Roy, S. S. Highly selective aptasensor for optical detection of whole cell gastrointestinal pathogen Shigella dysenteriae at label-free liquid crystal−aqueous interface. *Appl. Phys. Lett.* **2025**, *126*, No. 023703.

(9) Popov, P.; Mann, E. K.; Jákli, A. Thermotropic liquid crystal films for biosensors and beyond. *J. Mater. Chem. B* **2017**, *5*, 5061−5078.

(10) Shen, T.-Z.; Hong, S.-H.; Song, J.-K. Electro-optical switching of graphene oxide liquid crystals with an extremely large Kerr coefficient. *Nat. Mater.* **2014**, *13*, 394−399.
(11) Mertelj, A.; Lisjak, D.; Drofenik, M.; Copič, M. Ferromagnetism in suspensions of magnetic platelets in liquid crystal. *Nature* **2013**, *504*, 237−241.
(12) Ramezani-Dakhel, H.; Sadati, M.; Rahimi, M.; Ramirez-Hernandez, A.; Roux, B.; de Pablo, J. J. Understanding Atomic-Scale Behavior of Liquid Crystals at Aqueous Interfaces. *J. Chem. Theory Comput.* **2017**, *13*, 237−244.
(13) Sadati, M.; Apik, A. I.; Armas-Perez, J. C.; Martinez-Gonzalez, J.; Hernandez-Ortiz, J. P.; Abbott, N. L.; de Pablo, J. J. Liquid Crystal Enabled Early Stage Detection of Beta Amyloid Formation on Lipid Monolayers. *Adv. Funct. Mater.* **2015**, *25*, 6050−6060.
(14) Devadiga, D.; Ahipa, T. N. A review on the emerging applications of 4-cyano-4′-alkylbiphenyl (nCB) liquid crystals beyond display. *Mater. Sci. Eng., B* **2022**, *275*, No. 115522.
(15) Carlton, R. J.; Gupta, J. K.; Swift, C. L.; Abbott, N. L. Influence of Simple Electrolytes on the Orientational Ordering of Thermotropic Liquid Crystals at Aqueous Interfaces. *Langmuir* **2012**, *28*, 31−36.
(16) Carlton, R. J.; Ma, C. D.; Gupta, J. K.; Abbott, N. L. Influence of Specific Anions on the Orientational Ordering of Thermotropic Liquid Crystals at Aqueous Interfaces. *Langmuir* **2012**, *28*, 12796−12805.
(17) Hallett, J. E.; Hayward, D. W.; Arnold, T.; Bartlett, P.; Richardson, R. M. X-ray reflectivity reveals ionic structure at liquid crystal−aqueous interfaces. *Soft Matter* **2017**, *13*, 5535−5542.
(18) Allen, M. P. Molecular simulation of liquid crystals. *Mol. Phys.* **2019**, *117*, 2391−2417.
(19) Wilson, M. R.; Yu, G.; Potter, T. D.; Walker, M.; Gray, S. J.; Li, J.; Boyd, N. J. Molecular Simulation Approaches to the Study of Thermotropic and Lyotropic Liquid Crystals. *Crystals* **2022**, *12*, 685.
(20) Wilson, M. R. Progress in computer simulations of liquid crystals. *Int. Rev. Phys. Chem.* **2005**, *24*, 421−455.
(21) Wilson, M. R. Molecular simulation of liquid crystals: progress towards a better understanding of bulk structure and the prediction of material properties. *Chem. Soc. Rev.* **2007**, *36*, 1881−1888.
(22) Roscioni, O. M.; Muccioli, L.; Della Valle, R. G.; Pizzirusso, A.; Ricci, M.; Zannoni, C. Predicting the Anchoring of Liquid Crystals at a Solid Surface: 5-Cyanobiphenyl on Cristobalite and Glassy Silica Surfaces of Increasing Roughness. *Langmuir* **2013**, *29*, 8950−8958.
(23) Pizzirusso, A.; Berardi, R.; Muccioli, L.; Ricci, M.; Zannoni, C. Predicting surface anchoring: molecular organization across a thin film of 5CB liquid crystal on silicon. *Chem. Sci.* **2012**, *3*, 573−579.
(24) Ramezani-Dakhel, H.; Rahimi, M.; Pendery, J.; Kim, Y.-K.; Thayumanavan, S.; Roux, B.; Abbott, N. L.; de Pablo, J. J. Amphiphile-Induced Phase Transition of Liquid Crystals at Aqueous Interfaces. *ACS Appl. Mater. Interfaces* **2018**, *10*, 37618−37624.
(25) Roscioni, O. M.; Muccioli, L.; Zannoni, C. Predicting the Conditions for Homeotropic Anchoring of Liquid Crystals at a Soft Surface. 4-n-Pentyl-4′-cyanobiphenyl on Alkylsilane Self-Assembled Monolayers. *ACS Appl. Mater. Interfaces* **2017**, *9*, 11993−12002.
(26) Sadati, M.; Ramezani-Dakhel, H.; Bu, W.; Sevgen, E.; Liang, Z.; Erol, C.; Rahimi, M.; Taheri Qazvini, N.; Lin, B.; Abbott, N. L.; Roux, B.; Schlossman, M. L.; de Pablo, J. J. Molecular structure of canonical liquid crystal interfaces. *J. Am. Chem. Soc.* **2017**, *139*, 3841−3850.
(27) Chen, H.; Xu, C.; Xiao, G.; Chen, Z.; Yi, M.; Zhang, J. Surface anchoring behavior of 5CB liquid crystal confined between iron surfaces: A molecular dynamics study. *Appl. Surf. Sci.* **2020**, *508*, No. 145284.
(28) Szilvási, T.; Bao, N.; Yu, H.; Twieg, R. J.; Mavrikakis, M.; Abbott, N. L. The role of anions in adsorbate-induced anchoring transitions of liquid crystals on surfaces with discrete cation binding sites. *Soft Matter* **2018**, *14*, 797−805.
(29) Zhang, J.; Su, J.; Guo, H. An atomistic simulation for 4-cyano-4′-pentylbiphenyl and its homologue with a reoptimized force field. *J. Phys. Chem. B* **2011**, *115*, 2214−2227.
(30) Schmid, N.; Eichenberger, A. P.; Choutko, A.; Riniker, S.; Winger, M.; Mark, A. E.; Van Gunsteren, W. F. Definition and testing of the GROMOS force-field versions 54A7 and 54B7. *Eur. Biophys. J.* **2011**, *40*, 843−856.
(31) Berendsen, H. J. C.; Postma, J. P. M.; van Gunsteren, W. F.; Hermans, J. Interaction Models for Water in Relation to Protein Hydration. In *Intermolecular Forces*; Pullman, B., Ed.; Springer: Dordrecht, The Netherlands, 1981; pp 331−342.
(32) Abraham, M. J.; Murtola, T.; Schulz, R.; Páll, S.; Smith, J. C.; Hess, B.; Lindahl, E. GROMACS: High performance molecular simulations through multi-level parallelism from laptops to supercomputers. *SoftwareX* **2015**, *1*, 19−25.
(33) Bussi, G.; Donadio, D.; Parrinello, M. Canonical sampling through velocity rescaling. *J. Chem. Phys.* **2007**, *126*, No. 014101.
(34) Darden, T.; York, D.; Pedersen, L. Particle mesh Ewald: An N·log(N) method for Ewald sums in large systems. *J. Chem. Phys.* **1993**, *98*, 10089−10092.
(35) Essmann, U.; Perera, L.; Berkowitz, M. L.; Darden, T.; Lee, H.; Pedersen, L. G. A smooth particle mesh Ewald method. *J. Chem. Phys.* **1995**, *103*, 8577−8593.
(36) Hess, B. P-LINCS: A Parallel Linear Constraint Solver for Molecular Simulation. *J. Chem. Theory Comput.* **2008**, *4*, 116−122.
(37) Humphrey, W.; Dalke, A.; Schulten, K. VMD: visual molecular dynamics. *J. Mol. Graph.* **1996**, *14*, 33−38.
(38) Michaud-Agrawal, N.; Denning, E. J.; Woolf, T. B.; Beckstein, O. MDAnalysis: a toolkit for the analysis of molecular dynamics simulations. *J. Comput. Chem.* **2011**, *32*, 2319−2327.
(39) Gowers, R. J.; Linke, M.; Barnoud, J.; Reddy, T. J. E.; Melo, M. N.; Seyler, S. L.; Domanski, J.; Dotson, D. L.; Buchoux, S.; Kenney, I. M.; Beckstein, O. *MDAnalysis: A Python Package for the Rapid Analysis of Molecular Dynamics Simulation*; Los Alamos National Lab. (LANL): Los Alamos, NM (United States), **2019**. DOI: .
(40) Harris, C. R.; Millman, K. J.; van der Walt, S. J.; Gommers, R.; Virtanen, P.; Cournapeau, D.; Wieser, E.; Taylor, J.; Berg, S.; Smith, N. J.; et al. Array programming with NumPy. *Nature* **2020**, *585*, 357−362.
(41) Hunter, J. D. Matplotlib: A 2D Graphics Environment. *Comput. Sci. Eng.* **2007**, *9*, 90−95.
(42) Virtanen, P.; Gommers, R.; Oliphant, T. E.; Haberland, M.; Reddy, T.; Cournapeau, D.; Burovski, E.; Peterson, P.; Weckesser, W.; Bright, J.; et al. SciPy 1.0: fundamental algorithms for scientific computing in Python. *Nat. Methods* **2020**, *17*, 261−272.
(43) Kim, Y.-K.; Wang, X.; Mondkar, P.; Bukusoglu, E.; Abbott, N. L. Self-reporting and self-regulating liquid crystals. *Nature* **2018**, *557*, 539−544.
(44) Bahr, C. Surfactant-induced nematic wetting layer at a thermotropic liquid crystal/water interface. *Phys. Rev. E* **2006**, *73*, No. 030702.
(45) Roh, S.; Tsuei, M.; Abbott, N. L. Using Liquid Crystals for In Situ Optical Mapping of Interfacial Mobility and Surfactant Concentrations at Flowing Aqueous-Oil Interfaces. *Langmuir* **2021**, *37*, 5810−5822.
(46) Serrano, L. A.; Fornerod, M. J.; Yang, Y.; Gaisford, S.; Stellacci, F.; Guldin, S. Phase behaviour and applications of a binary liquid mixture of methanol and a thermotropic liquid crystal. *Soft Matter* **2018**, *14*, 4615−4620.
(47) Bedolla Pantoja, M. A.; Abbott, N. L. Surface-Controlled Orientational Transitions in Elastically Strained Films of Liquid Crystal That Are Triggered by Vapors of Toluene. *ACS Appl. Mater. & Interfaces* **2016**, *8*, 13114−13122.

https://doi.org/10.1021/acsomega.5c05516
ACS Omega 2025, 10, 61288−61295